MATHEMATICAL MODELING
IN PHYSICS AND ENGINEERING

Częstochowa 2021

The conference Mathematical Modeling in Physics and Engineering – MMPE'21 is organized by Czestochowa Branch of Polish Mathematical Society jointly with the Department of Mathematics of Czestochowa University of Technology.

Mathematical modeling is at the core of contemporary research within a wide range of fields of science and its applications. The MMPE'21 focuses on various aspects of mathematical modeling and usage of computer methods in modern problems of physics and engineering. The goal of this conference is to bring together mathematicians and researchers from physics and diverse disciplines of technical sciences. The conference participants represent a prominent group of recognized scientists as well as young researchers and PhD students. This time we have speakers from University of Lodz, Technical University of Košice, Gdansk University of Technology and Czestochowa University of Technology.

This year the conference is organized for the 12th time. Due to the COVID-19 pandemic the Organizing Committee decided to hold the event online to ensure all participants may meet safely.

Organizers

CONTENTS

APPROXIMATION OF THE RIESZ-CAPUTO FRACTIONAL DERIVATIVE OF VARIABLE ORDER

Tomasz Blaszczyk [1], Krzysztof Bekus [2], Krzysztof Szajek [3], Wojciech Sumelka [4]

[1,2]Department of Mathematics, Czestochowa University of Technology, Czestochowa, Poland
[3,4]Institute of Structural Analysis, Poznan University of Technology, Poznan, Poland
[1]tomasz.blaszczyk@pcz.pl, [2]krzysztof.bekus@im.pcz.pl, [3]krzysztof.szajek@put.poznan.pl, [4]wojciech.sumelka@put.poznan.pl

Keywords: **Riesz-Caputo derivative, variable order, numerical integration**

In the last few decades, the fractional differential equations have become a relatively flexible modelling tool especially when strong scale-effect appears [1]. In most applications of the fractional calculus, the order of differential/integral operators is assumed to be fixed along the analysed process. However, new interesting possibilities arise when we consider the order of the fractional derivatives or/and integrals not constant over the process but to be a spatial variable function $\alpha(x)$.

The most common fractional operators studied in the literature are left-sided derivatives taking into account a long memory characteristic (they accumulate all the 'historical' data). Recently, several researchers develop a theory where both fractional operators are taken into account, like the Riesz–Caputo fractional derivative [2] or the fractional differential operator being a composition of the left and right fractional derivatives [3].

In this work, we are studied the following Riesz-Caputo fractional derivative of variable order with α depending on space variable [4]

$$ {}^{RC}_{x-\ell}D^{\alpha(x)}_{x+\ell} f(x) = \frac{1}{2}\left({}^{C}_{x-\ell}D^{\alpha(x)}_{x} f(x) + (-1)^{n} {}^{C}_{x}D^{\alpha(x)}_{x+\ell} f(x)\right) \tag{1} $$

Operators ${}^{C}_{x-l}D^{\alpha(x)}_{x}$ and ${}^{C}_{x}D^{\alpha(x)}_{x+\ell}$ are well known fractional Caputo derivatives, with fixed memory length ℓ and variable order $\alpha(x) > 0$, defined as

$$ {}^{C}_{x-l}D^{\alpha(x)}_{x} f(x) = \frac{1}{\Gamma(n-\alpha(x))}\int_{x-l}^{x} (x-\tau)^{n-\alpha(x)-1} f^{(n)}(\tau) d\tau \tag{2} $$

$$ {}_{x}^{C}D_{x+\ell}^{\alpha(x)} f(x) = \frac{(-1)^n}{\Gamma(n-\alpha(x))} \int_{x}^{x+\ell} (\tau - x)^{n-\alpha(x)-1} f^{(n)}(\tau) d\tau \tag{3} $$

During the presentation a few modified classical numerical integration methods, for the approximate computation of the Riesz-Caputo derivative (1) will be presented. The proposed methods are based on polynomial interpolation. Obtained numerical results will be compared with the exact ones (received by using series representation of the Riesz-Caputo derivative [5]). Additionally, the experimental rate of convergence will be estimated for discussed approximations.

This work is supported by the National Science Centre, Poland under Grant No. 2017/27/B/ST8/00351.

References

[1] Sumelka W., Voyiadjis G.Z., A Hyperelastic Fractional Damage Material Model with Memory, International Journal of Solids and Structures 124 (2017), 151-160.

[2] Szajek K., Sumelka W., Blaszczyk T., Bekus K., On selected aspects of space-Fractional Continuum Mechanics model approximation, International Journal of Mechanical Sciences 167 (2020), 105287.

[3] Blaszczyk T., Analytical and Numerical Solution of the Fractional Euler-Bernoulli Beam Equation, Journal of Mechanics of Materials and Structures 12(1) (2017), 23-34.

[4] Blaszczyk T., Bekus K., Szajek K., Sumelka W., Approximation and application of the Riesz-Caputo fractional derivative of variable order with fixed memory, Meccanica (2021). https://doi.org/10.1007/s11012-021-01364-w

[5] Blaszczyk T., Bekus K., Szajek K., Sumelka W., On numerical approximation of the Riesz-Caputo operator with the fixed/short memory length, Journal of King Saud University - Science 33(1) (2021), 101220.

FAILURES IN OVERLOADED POWER GRIDS

Zbigniew Domanski

Department of Mathematics, Czestochowa University of Technology, Czestochowa, Poland
zbigniew.domanski@im.pcz.pl

Keywords: **failure, power grids, statistics**

The growing diversity of multicomponent systems raises questions about the reliability and yield of these systems under progressive loadings. From the operational point of view, the most intriguing question is how the properties of individual components combine to produce the overall performance of the system to which they belong. This question is important because under parallel load units become overloaded and fail. These failures trigger subsequent over loadings which reduce the system performance or eventually lead to a catastrophic avalanche of failures. Such a catastrophe happens because systems subjected to an increasing load begin to fail when the internal load exceeds the critical value of less reliable units.

An important class of multicomponent systems includes power grids. Typical power grids, such as distribution networks, combine thousands of components that are interconnected according to specified geometries represented by graphs. Especially, the small-world topology is reported as present and beneficial in large-scale installations involving nationwide power systems as well as medium or small power grids. Particularly, in smart grids of renewable energy sources, such as small-scale photovoltaic systems or small-wind turbines, the small world topology turns out to be beneficial. For example, networks with small-world connectivity can significantly enhance their robustness against different attacks by a simultaneous increase of the rewiring probability and average degree.

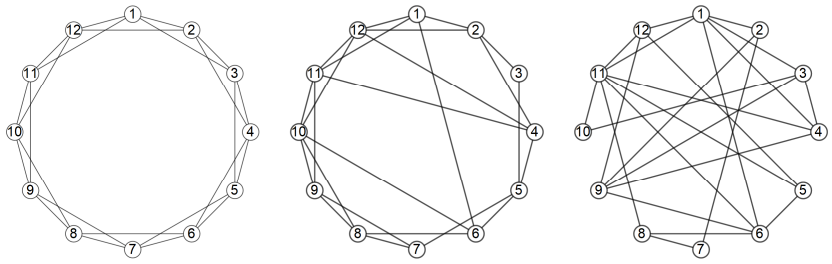

Fig. 1. Exemplary small-world networks: from a regular ring lattice to a random lattice.

We apply the fibre bundle model to analyse the highest load supported by a given power system when the system's topology is perturbed. To collect data necessary to build statistical models we employ two families of graphs, whose nodes represent components of power grids. Specifically, we use the Watts-Strogatz model to generate small-world-like networks, whereas the second family involves the Erdos-Renyi graphs. Each power grid component is represented by a random variable that reflects the value of load supported safely by the component. In our simulations, a sequence of stepwise growing values of the external load gives the maximal value of load that the given system sustains and thus allows us to obtain data for different system sizes and different graphs. Due to the simulations, we have determined numerically effective distributions of maximal loads in hypothetical power grids. By fitting discrete distributions of maximal loads, we have found how the random component-load-thresholds influence the macroscopic yield of the power grid.

References

[1] Domanski Z., Spreading of Failures in Small-World Networks: A Connectivity-Dependent Load Sharing Fibre Bundle Model, Frontiers in Phys. 2020, 8, id 552550.

[2] Newman M., The structure and function of complex networks, SIAM Rev. 2003, 45, 167-256

[3] Cuadra L., Salcedo-Sanz S., Del Ser J., Jimenez-Fernandez S., Geem Z., A critical review o robustness in power grids using complex networks concepts, Energies 2015, 8, 9211-9265.

[4] Rosas-Casals M., Valverde S., Sole R. V., Topological vulnerability of the European power grid under errors and attacks, Int. J. of Bifurcation and Chaos 2007, 17, 2465-2475.

[5] Sun Y., Tang X., Zhang G., Miao F., Wang P., Dynamic power flow cascading failure analysis of wind power integration with complex network theory, Energies 2017, 11, 63.

THE REWARD FOR A GOOD DECISION VS PUNISHMENT FOR THE WRONG ONE – HOW IT WORKS IN MACHINE LEARNING-BASED CLASSIFICATION

Andrzej Z. Grzybowski

Department of Mathematics, Czestochowa University of Technology, Czestochowa, Poland
andrzej.grzybowski@pcz.pl

Keywords: **ordinal classification, classification error costs, evolutionary learning**

Classification problems consist in identifying the most probable class c an instance v (usually represented by its feature vector $\mathbf{x}$) belongs to. Classification problems are at the core of the field of machine learning. They have been researched intensively over the last decades. In literature, one can find great many different classifiers developed under different assumptions about the classification problems as well as by the adoption of different learning algorithms, e.g. [1], [2]. However, after studying many classification problems of different types and nature, it is clear to the machine-learning community that there is no single classification algorithm that is superior with all respects and for all datasets [3], a conclusion analogous to famous no free lunches theorem in the theory of stochastic search and optimization [4]. On the other hand, it appears that some learning algorithms outperform others for some specific problems and/or types of data. In this paper we focus on the ordinal classification problems, i.e. problems where the class label (target variable) takes on values in a set C of categories that exhibit a natural ordering. We consider multiclass problems, it is the case where the number k of classes is greater than 2. Then we have $k(k-1)$ different classification errors with, possibly, different consequences. To each of those errors, it is assigned its specific error cost (weight) that represents the importance of its repercussions. An index of performance of a classifier is defined as the expected value of the classification-result-cost, and consequently, the learning algorithms are aimed at finding a classifier that minimizes such an index. However, due to the fact that the optimality criterion cannot be expressed by any closed-form-mathematical expression and the value of the criterion can only be evaluated for each specific classifier separately, the minimization problem cannot be solved directly. Moreover, it implies that when looking for the expected cost minimum we have to confine ourselves to gradient-free optimization methods. Thus in presented studies global optimization (GO) methods that are based on the idea of the stochastic search are proposed to cope with such a task. We use computer simulations to study the performance of some popular stochastic global optimization methods as learning tools for some specific type of ordinal classification problems. Some

remarks about the impact of the error-cost-matrix on the probabilities of a particular error occurrence are formulated as well.

Based on our simulation results one can conclude that among considered GO algorithms, the Genetic Algorithm (GA) is the best one as a tool for classifier-learning tasks in the ordinal classification problems. The GA performs really well - the average probability of correct classification of an instance is about 0.9 and one hardly can expect a higher frequency of correct decisions in such uncertain decision problems. Our simulations show that these probabilities of success decrease when the number of classes increases – a rather intuitive observation. However, it is worth noticing that, in spite of this perhaps natural tendency, the supremacy of the GA over the remaining learning algorithms gets more evident when the number of classes increases. But one should be aware that in problems with unequal costs of classification errors, the probabilities of correct classification are not necessarily the most crucial ones. It is worth emphasizing that, instead, sometimes it is even more important not to make specific classification errors (in a given specific problem). In such cases one should focus on the weight matrix - proper construction of the matrix is of primary interest in all classification problems with unequal costs of misclassification errors. Our simulation experiments revealed some important facts about the influence of the weight matrix on the classifier-learning results. The results that we have obtained during our simulations confirm that the proportions between the weights of particular classification errors have a proper impact on the proportions between corresponding probabilities of errors and, again, the GA learning algorithm is the best with respect to this issue. It was also shown, that the weights assigned to correct classifications are also very important, they make it easier for the learning algorithm to lower the probabilities of misclassification. Thus, the role of both the reward and punishment revealed by our results concerning machine learning is in line with the operant-conditioning principle formulated by Skinner to explain the human-learning nature, [5].

References

[1] Mane S., Sonawani, S. S., Sakhare S., and Kulkarni, P. V., (2014), ”Multi-objective Evolutionary Algorithms for Classification: A Review”, International Journal of Application or Innovation in Engineering and Management, 292-297

[2] Espejo, P.G., Ventura, S., Herrera, F., (2010) ”A Survey on the Application of Genetic Programming to Classification”, IEEE Transactions On Systems, Man, And Cybernetics-Part C: Applications And Reviews, Vol. 40, No. 2, 121-144

[3] Wolpert, D.H. (1996), ”The lack of a priori distinctions between learning algorithms.”, Neural computation 8(7), 1341-1390

[4] Spall, J.C.: Introduction To Stochastic Search And Optimization; Estimation, Simulation, And Control , John Wiley and Sons. Inc., Publication, 2003.

[5] McLeod, S. A. (2018). ”Skinner - operant conditioning.”, Retrieved from https://www.simplypsychology.org/operant-conditioning.html (accessed 14.06.2019)

SOLVING THE PROBLEM OF THERMAL CONTACT CONDUCTANCE WITH A TIME DERIVATIVE IN CONJUGATION CONDITION USING THE POTENTIAL METHOD

Bohdan Kopytko [1]***, Roman Shevchuk*** [2]

[1] *Department of Mathematics, Czestochowa University of Technology, Czestochowa, Poland*
[2]*Institute of Applied Mathematics and Fundamental Sciences, Lviv Polytechnic National University, Lviv, Ukraine*
[1]*bohdan.kopytko@pcz.pl,* [2]*r.v.shevchuk@gmail.com*

Keywords: **parabolic potential, Feller semigroup**

Consider the strip

$$S_t = \{(s,x):\ 0 \le s < t \le T,\ -\infty < x < \infty\}$$

in the Euclidean space $\mathbb{R}^2$ of variables (s,x) (T >0 fixed) and two domains

$$S_t^{(1)} = \{(s,x):\ 0 \le s < t \le T,\ -\infty < x < r(s)\}$$

and

$$S_t^{(2)} = \{(s,x):\ 0 \le s < t \le T,\ r(s) < x < \infty\}$$

in it, where $x = r(s)$, $s \in [0,T]$, is a given function which belongs to the Hölder class $H^{1+\frac{\alpha}{2}}([0,T])$, $0 < \alpha < 1$ (see, e.g., [1, Ch. I, §1]).

Below we will use the following notations: $D_{1s} = (-\infty, r(s))$, $D_{2s} = (r(s), \infty)$; $C_b(\mathbb{R})$ denotes the Banach space of bounded and continuous on $\mathbb{R}$ functions with the norm

$$\|\varphi\| = \sup_{x \in \mathbb{R}} |\varphi(x)|;$$

if Q is the domain in the space $\mathbb{R}^2$ of points (s,x) and $\overline{Q}$ is the closure of this domain, then $C^{m,l}(Q)$ ($C^{m,l}(\overline{Q})$), where m and l are nonnegative integers, denote the sets of continuous functions on Q ($\overline{Q}$) for which there exist continuous partial derivatives with respect to s and x up to orders m and l, respectively ($C^{0,0}(Q) = C(Q)$).

Consider the following conjugation problem: find a classical solution $u(s,x,t),\ 0\le s\le t\le T,\ x\in\mathbb{R},$ of the heat equation

$$\frac{\partial u}{\partial s}+\frac{1}{2}\frac{\partial^2 u}{\partial x^2}=0,\ (s,x)\in S_t^{(i)},\ i=1,2, \tag{1}$$

which satisfies the "initial" condition

$$\lim_{s\uparrow t} u(s,x,t)=\varphi(x),\ x\in\mathbb{R}, \tag{2}$$

and two conjugation conditions

$$u(s,r(s)-0,t)=u(s,r(s)+0,t),\ 0\le s\le t\le T, \tag{3}$$

$$\begin{aligned}&\sigma(s)\frac{\partial u}{\partial s}(s,r(s),t)+q_1(s)\frac{\partial u}{\partial x}(s,r(s)-0,t)-\\&-q_2(s)\frac{\partial u}{\partial x}(s,r(s)+0,t)=0,\ 0\le s<t\le T,\end{aligned} \tag{4}$$

where $\varphi(x),\ x\in\mathbb{R},\ \sigma(s),\ q_1(s),\ q_2(s),\ s\in[0,T]$ are given continuous functions; furthermore, $\varphi\in C_b(\mathbb{R}),\ \sigma\ge 0,\ q_1\ge 0,\ q_2\ge 0$ and $\sigma+q_1+q_2\ne 0.$ Here $u(s,r(s)-0,t)$ $\left(\frac{\partial u}{\partial x}(s,r(s)-0,t)\right)$ and $u(s,r(s)+0,t)$ $\left(\frac{\partial u}{\partial x}(s,r(s)+0,t)\right)$ denote the limits of the function $u(s,x,t)$ $\left(\frac{\partial u}{\partial x}(s,x,t)\right)$ at $(s,r(s))$ as the point (s,x) tends to $(s,r(s))$ from the side of the domains $S_t^{(1)}$ and $S_t^{(2)}$ respectively.

Note that the problem concerning the classical solvability of (1)-(4) appears, in particular, in the theory of diffusion processes when studying, by using the analytical methods, the so-called problem of pasting together two diffusion processes on a line (see, e.g., [2] and [3]). In these and in some other our papers the described problem is considered (including in a more general setting) under the assumption that the common boundary of the domains $S_t^{(1)}$ and $S_t^{(2)}$ is defined by the relation $x=r(s)\equiv r,\ s\in[0,T],$ where r is a positive constant.

Here, the problem (1)-(4) is considered for the case of curvilinear domains $S_t^{(i)}$, $i=1,2,$ under the condition that $\sigma\ne 0.$

We prove the following theorem:

Theorem. Assume that r and φ belong to the spaces $H^{1+\frac{\alpha}{2}}([0,T])$ and $C_b(\mathbb{R})$ respectively. Assume also that the functions σ, q_1, q_2 are continuous in $s\in[0,T]$ and $\sigma>0,\ q_1\ge 0,\ q_2\ge 0.$ Then the conjugation problem (1)-(4) has a unique solution

$$u \in C(\overline{S}_t) \cap C^{1,2}(S_t)$$

for which the estimate

$$|u(s,x,t)| \leq c\|\varphi\|$$

holds, and this solution can be represented in the form

$$u(s,x,t) = \int_{\mathbb{R}} g(s,x,t,y)\varphi(y)dy + \int_s^t g(s,x,\tau,r(\tau))V(\tau,t)d\tau,$$

where g is the fundamental solution of the equation (1), V is the solution of some Volterra integral equation of the second kind and c is a constant.

Furthermore, we prove that, using the solution of the problem (1)-(4), one can define the two-parameter Feller semigroup which describes some inhomogeneous Feller process on a real line. Some additional properties of the constructed process are also studied.

References

[1] Ladyzhenskaya O.A., Solonnikov V.A., Ural'tseva N.N., Linear and Quasilinear Equations of Parabolic Type, Nauka, Moscow 1967 (in Russian).

[2] Kopytko B.I., Portenko M.I., The problem of pasting together two diffusion processes and classical potentials, Theory Stoch. Process. 2009, 15(2), 126-139.

[3] Kopytko B.I., Shevchuk R.V., On pasting together two inhomogeneous diffusion processes on a line with the general Feller-Wentzell conjugation condition, Theory Stoch. Process. 2011, 17 (2), 55-70.

FRACTIONAL HEAT CONDUCTION IN A COMPOSITE SOLID CYLINDER SUBJECTED TO A HEAT SOURCE

Stanisław Kukla [1]***, Urszula Siedlecka*** [2]

[1,2]*Department of Mathematics, Czestochowa University of Technology, Czestochowa, Poland*
[1]*stanislaw.kukla@pcz.pl,* [2]*urszula.siedlecka@pcz.pl*

Keywords: **fractional heat conduction, Caputo derivative**

Fractional calculus in mathematical modelling of the heat conduction was applied in many papers, for instance in the papers [1-4] the models with fractional derivatives were used. The subject of this contribution is an analysis of the effect of the derivative fractional order on the temperature distribution in a cylinder with a heat source. The object under consideration is composite cylinder consisting of inner solid cylinder and an outer concentric layer (Fig. 1). The heat conduction is governed by fractional heat equation with the Caputo time-derivative [1]

$$\nabla^2 T_i(t,r,z)+\frac{1}{\lambda_i}g_i(t,r,z)=\frac{1}{a_i}\frac{\partial^\alpha T_i}{\partial t^\alpha}(t,r,z),\quad z\in[0,H],\ r\in[r_{i-1},r_i],\ i=1,2 \tag{1}$$

where λ_i is the thermal conductivity, a_i is the thermal diffusivity, $g_i(t,r,z)$ is the volumetric energy generation, α denotes the fractional order of the Caputo derivative [2] with respect to time t, ∇^2 is the Laplace operator and $r_0=0$.

We assume the boundary conditions, the conditions of perfect thermal contact at interface ($r=r_1$) and the initial condition in the following form

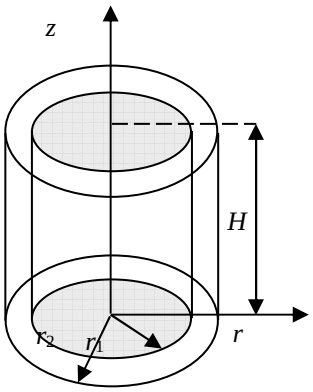

Fig. 1. A sketch of the considered finite cylinder

$$\left|T_1(t,0,z)\right| < \infty \tag{2}$$

$$\lambda_2 \left.\frac{\partial T_2}{\partial r}\right|_{r=r_2} = a_\infty \left(T_\infty(t) - T_2(t,r_2,z)\right) \tag{3}$$

$$\left.\frac{\partial T_i}{\partial z}\right|_{z=0} = 0, \quad \left.\frac{\partial T_i}{\partial z}\right|_{z=H} = 0, \quad i = 1,2 \tag{4}$$

$$T_1(t,r_1,z) = T_2(t,r_1,z), \quad \lambda_1 \left.\frac{\partial T_1}{\partial r}\right|_{r=r_1} = \lambda_2 \left.\frac{\partial T_2}{\partial r}\right|_{r=r_1} \tag{5}$$

$$T_i(0,r,z) = F_i(r,z), \quad i = 1, 2 \tag{6}$$

where a_∞ is the heat transfer coefficient and T_∞ is the ambient temperature.

To obtain the fractional equation with a homogeneous boundary conditions, we introduce new functions $\psi_i(t,r,z)$ given as

$$\psi_i(t,r,z) = T_i(t,r,z) - T_\infty(t), \quad i = 1, 2 \tag{7}$$

An analytical solution of the boundary-initial problem for the functions ψ_i has been obtained in the form of double series of eigenfunctions

$$\psi_i(t,r,z) = \sum_{m=0}^{\infty}\sum_{n=1}^{\infty} \theta_{m,n}(t) R_{i,m,n}(r) Z_m(z), \quad i = 1, 2 \tag{8}$$

where $R_{i,m,n}(r)$ and $Z_m(z)$ are received as solutions of corresponding eigenproblems, $\theta_{m,n}(t)$ is a solution of the time-fractional non-homogenous differential equation. Numerical calculations of the temperature distribution in the considered cylinder are presented.

References

[1] Kukla S., Siedlecka U., Time-fractional heat conduction in a finite composite cylinder with heat source, Journal of Applied Mathematics and Computational Mechanics 2020, 19 (2), 85-94.

[2] Povstenko Y., Klekot J., Time-fractional heat conduction in two joint half-planes. Symmetry 2019, 11 (6), 800.

[3] Ciesielski M., Blaszczyk T., An exact solution of the second order differential equation with the fractional/generalised boundary conditions. Advances in Mathematical Physics 2018, 7283518.

[4] Siedlecka U., Heat conduction in a finite medium using the fractional single-phase-lag model, Bulletin of the Polish Academy of Sciences, Technical Sciences 2019, 67 (2), 401-407.

MODELING ELECTRICAL ACTIVITY OF NEURONS

Frank Fernando Llovera Trujillo [1]***, Justyna Signerska-Rynkowska*** [2]

[1]*Gdansk University of Technology,*
Gdansk, Poland
[2]*Institute of Applied Mathematics, Gdansk University of Technology,*
Gdansk, Poland

Keywords: **Chialvo model, bifurcation, chaos.**

The problem of modeling neuronal activity to capture and reproduce accurately neurons behavior has resulted extremely challenging. Many models have been proposed to address this problem, starting from the Hodgkin-Huxley(HH) system, presented in 1952 in the form of an extremely complex four-dimensional phase space dynamical system, that although can be considered a foundation of neuronal modeling has a high level of complexity, to more modern variants such as the FitzHugh-Nagumo (FHN) or Morris-Lecar (Morris and Lecar, 1981).

The idea of being able to simplify these models has lead to experiment with more simple and treatable discrete-time systems in the form of point maps: the map-based models. Some of the most renowned ones, in one and two dimensions are: a modified FitzHugh-Nagumo system with a recovery variable used as a simple model of excitable neuron generating spikes; Aguirre-Campos-Pascual-Serrano model (2006), a map with two different branches for modeling spiking-bursting; Rulkov model (2002) and Courbage-Nekorkin-Vdovin model (2007), among others.

In 1995, Dante R. Chialvo presented a 2D model for neural excitability ([2]). We have decided to focus our work in this model, given that most of the results related to it had a numerical or intuitive nature.

The model takes the form:

$$x_{n+1} = f(x_n, y_n) = x_n^2 \exp(y_n - x_n) + k \tag{1a}$$

$$y_{n+1} = g(x_n, y_n) = a y_n - b x_n + c \tag{1b}$$

where x is a membrane voltage-potential (the most important dynamical variable in all the neuron models) and y is so-called recovery variable. The time-constant $a \in (0,1)$, the activation dependence $b \in (0,1)$ and the offset c > 0 are the real

parameters connected with the recovery process. In turn, $k \geq 0$ can be interpreted as a time-dependant perturbation of the voltage.

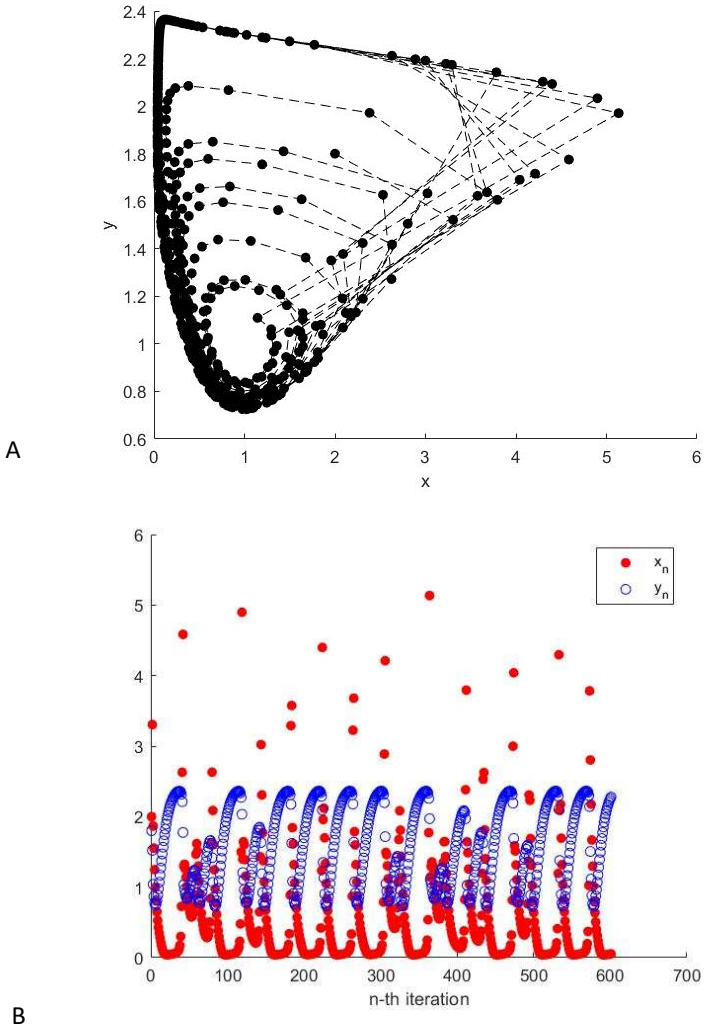

Figure 1: A trajectory of a 2D- Chialvo model in (x,y)-phase space (A) and a corresponding voltage (filled circle) and a recovery- variable (empty circle) time plots (B). Parameters: $k = 0.03, a = 0.89, b = 0.18, c = 0.28$.

The 1-dimensional subsystem:

$$x_{n+1} = f(x_n, r) = x_n^2 \; exp(r - x_n) + k \tag{2}$$

Where $r \in \mathbb{R}$ is a parameter, is called the 1-dimensional (1D) Chialvo model.

If $b \ll 1$, the system (1a) - (1b) can be seen as a *slow-fast* (discrete) system, where the voltage variable x and the recovery variable y, can be referred to as *fast* and *slow* variables, respectively. Consequently, while x_n describes spiking behavior, y_n acts as a slowly changing parameter (with time-scale variation $\varepsilon \ll 1$) that modulates the spiking dynamics. Such models can be analized by firstly treating (2) as a quazi-static approximation of (1a) - (1b) with parameter $r \equiv y$. If for some values of r (2) exhibits equilibrium dynamics (due to the existence of a stable fixed point) and for some other values it exhibits periodic dynamics (due to the existence of a stable periodic orbit), then bursting in the system (1a) - (1b) occurs because slowly varying y_n acts as bifurcation parameter that makes the dynamics of x switching between these two regimes (similar approach can be applied for ODE bursting systems, compare e.g. with [8]). Therefore bursting behaviour in the above neuron model is indeed directly connected with the types of bifurcations present in the fast system (2).

Origin and classification of bursting types in neurons (i.e. the repeating episodes when a few spikes occur in a rapid succession followed by a quiescence period) is a significant problem in neurophysiology of neurons. In order to characterize bursting dynamics of the Chialvo model (1a)-(1b), we study the existence and stability of fixed points and corresponding bifurcations in one-dimensional Chialvo model (2), i.e. showing that it produces fold bifurcation and flip bifurcation, which next are linked with Izhikevich and Hoppensteadt classification of bursting mappings ([6]).

In particular, we rigorously prove that the system undergoes flip and saddle-node bifurcations. As an illustration of our results, we show below how the 1D Chialvo model undergoes a periodic flip bifurcation when $k = 0$ at $x_0 = 3$ and $r_0 = 3 - \ln(3)$.

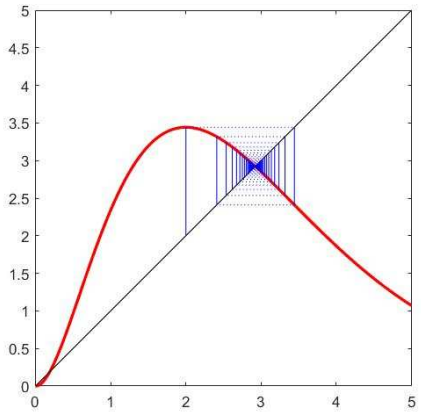

A

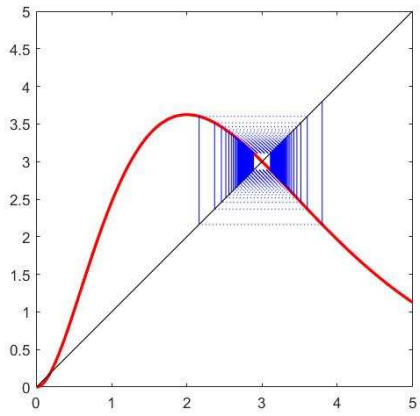

B

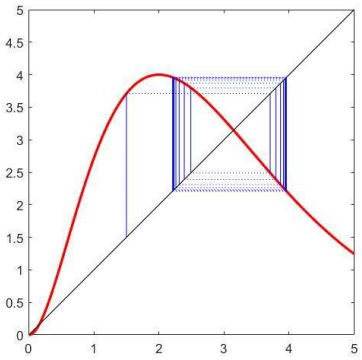

C

Figure 2: Cobweb diagrams for 1D Chialvo model and $k = 0$ using 150 iterations and initial point x_i Panel A: $r = 1.85, x_i = 1.5$, Panel B: $r = 3 - \ln(3)$ (flip bifurcation value), $x_i = 4$, Panel C: $r = 2, x_i = 1.5$

Finally, we show that a map $f(x_n, r)$, independently of the value of parameter r, is an *S- unimodal* map (i.e. a unimodal maps with negative Schwarzian derivative). Since the theory of such maps is well-developed, we are able to prove uniqueness of attracting periodic orbits and describe chaotic behaviour, relevant for the classification of bursting neurons, with the existence of the absolutely continuous invariant probability measure (acip) with negative Lyapunov exponent almost everywhere (for some r values), which can be identified with some strong dependence on initial conditions.

References

[1] Z. Jing, J. Yang, W. Feng Bifurcation and chaos in neural excitable system, Chaos Solitons & Fractals 27, no. 1, 197–215 (2006)
[2] D.R. Chialvo Generic excitable dynamics on a two-dimensional map, Chaos, Solitons & Fractals 5, no. 3–4, 461–479 (1995)
[3] E.M. Izhikevich, Neural excitability, spiking, and bursting, Internat. J. Bifur. Chaos Appl. Sci. Engrg. 10, no 6, 1171–1266 (2000)
[4] Y.A. Kuznetsov, Elements of applied bifurcation theory. Third edition. Applied Mathematical Sciences, 112. Springer-Verlag, New York, 2004
[5] H. Thunberg, Periodicity versus Chaos in One-Dimensional Dynamics. SIAM Review 43, no 1, 3–30 (2001)
[6] E.M. Izhikevich, F. Hoppensteadt, Classification of bursting mappings., Internat. J. Bifur.Chaos Appl. Sci. Engrg. 14, no 11, 3847–3854 (2004)
[7] H. Thunberg, Periodicity versus Chaos in One-Dimensional Dynamics. SIAM Review 43, no. 1, 3–30 (2001)
[8] J. Rinzel, A formal classification of bursting mechanisms in excitable systems. Third edition. Mathematical Topics in Population Biology, Morphogenesis and Neurosciences, eds E.Teramoto & M. Yamaguti, Lecture Notes in Biomathematics, Vol. 71, Springer- Verlag, Berlin, 1987

VOLUME FORM, VECTOR PRODUCT AND THE DIVERGENCE THEOREM

Antoni Pierzchalski

Faculty of Mathematics and Computer Science, University of Lodz
Lodz, Poland
antoni.pierzchalski@wmii.uni.lodz.pl

Keywords: **scalar product, vector product, volume form, the divergence, the divergence theorem**

It is about the divergence theorem – a one of the most important results in modern calculus with a wide spectrum of applications. For example, the known Archimedean principle saying that the buoyant force acting on an object immersed in a fluid is equal to the weight of the fluid displaced by the object, is simply one of its version (cf. [1]). On the other hand the divergence theorem is just a version of the Stokes theorem. Its unusualness come from the fact that it deals with a vector field. Vector fields represent a displacement of forces acting on a physical body. In practice, the values of the displacement can be measured exactly at the boundary only. The divergence theorem gives then some information on what is going inside. The vector character of the force makes that many nontrivial boundary conditions can be formulate when solving a boundary value problem. For example in the theory of elastic body there are the four natural boundary conditions: Dirichlet, Absolute, Relative and Neuman (cf. [2]).

Let us introduce some notions and facts that are necessary in formulating the divergence theorem and its generalizations.

The Cartesian space R^n is naturally equipped with some additional structures.

First of all, with the Euclidean scalar product.

For a fixed point p in R^n , the *scalar product* is a function g that subordinates - to any two vectors hooked at p - a real number.

With respect to its vector arguments the function is

(a) bilinear,

(b) symmetric,

(c) positively defined.

In the Cartesian space R^n the canonical scalar product of two vectors is defined as the sum of products of their coordinates:

$$g_{can}(\boldsymbol{v},\boldsymbol{w})=v_1w_1+\ldots+v_nw_n$$

The system of n-vectors of the ordered canonical base in R^n

$$\boldsymbol{e_1,\ldots,e_n}$$

is orthonormal with respect to the product $g=g_{can}$, i.e.,

$$g(\boldsymbol{e_i,e_j})= \delta_{ij} \quad (\delta_{ij}=0 \text{ for } i\neq j \text{ and } \delta_{ij=1} \text{ for } i=j),$$

The next natural structure is the Euclidean volume form.

The *volume form* is a function Ω that subordinates to any ordered system of *n* vectors hooked at *p* a real number.

With respect to its vector arguments the function is

(d) n-linear

(e) skew-symmetric

(f) nondegenerate

In the Cartesian space R^n the action of canonical volume form on *n*-vectors is defined as their determinant:

$$\Omega_{can}(\boldsymbol{v_1,\ldots,v_n})=\det(\boldsymbol{v_1,\ldots,v_n})$$

i.e., as the determinant of the matrix composed from vectors of the system as its rows (columns).

On the system of *n*-vectors of the ordered canonical base the value of the volume form $\Omega = \Omega_{can}$ equals 1, i.e.,

(g) $$\Omega(\boldsymbol{e_1,\ldots,e_n})=1.$$

The canonical structures *g* and Ω do not depend on the point *p*. In the practical and technical application there is a need yet to consider g and Ω as functions depending on *p* to expose e.g., inhomogeneity of the investigated medium (domain, object, material). The only demand then is that *g* should fulfil the conditions (a)-(c). The demands on Ω are then the conditions (d)-(f) and, additionally, the normalizing condition (g) that should be satisfied by any suitably ordered base $\boldsymbol{e_1,\ldots,e_n}$, orthonormal with respect to the given *g*.

Assume now that we have a domain *D* in R^n equipped with scalar product *g* and a volume form Ω satisfying conditions (a)-(g). We can define then the third structure:

Fix a point *p* in D. *The vector product* is a function that subordinates to any ordered system of (*n-1*)-vectors $\boldsymbol{v_1,\ldots,v_{n-1}}$ hooked at *p* the vector $\boldsymbol{v_1}\times\ldots\times\boldsymbol{v_{n-1}}$ also hooked at *p* as follows:

Fix vectors $\boldsymbol{v_1,\ldots,v_{n-1}}$. The function

$$\boldsymbol{v} \rightarrow \Omega(\boldsymbol{v,v_1,\ldots,v_{n-1}})$$

defines a linear functional on the linear space of all vectors hooked at p. By the Riesz theorem the functional is represented by a vector. More explicitly, there exists a unique vector hooked at p – call it $\boldsymbol{v}_1\times\ldots\times\boldsymbol{v}_{n-1}$ – representing the functional, i.e., satisfying

$$g(\boldsymbol{v},\, \boldsymbol{v}_1\times\ldots\times\boldsymbol{v}_{n-1})= \Omega(\boldsymbol{v},\boldsymbol{v}_1,\ldots,\boldsymbol{v}_{n-1}).$$

With respect to its vector arguments the vector product is

(h) (n-1)-linear

(i) skew-symmetric.

Moreover,

(j) the vector $\boldsymbol{v}_1\times\ldots\times\boldsymbol{v}_{n-1}$ *is g-orthogonal to each of the arguments* $\boldsymbol{v}_1,\ldots,\boldsymbol{v}_{n-1}$, *i.e.,* $g(\boldsymbol{v}_1\times\ldots\times\boldsymbol{v}_{n-1}, \boldsymbol{v}_i)=0$, *for* $\boldsymbol{i}=1,\ldots,n-1$,

(k) the length $|\boldsymbol{v}_1\times\ldots\times\boldsymbol{v}_{n-1}|$ *of* $\boldsymbol{v}_1\times\ldots\times\boldsymbol{v}_{n-1}$ *is equal to the (n-1)-dimensional measure (volume) of the parallelogram spanned by vectors* $\boldsymbol{v}_1,\ldots,\boldsymbol{v}_{n-1}$. *In particular, it is equal zero if and only if the vectors are linearly dependent.*

(l) For any system of vectors $\boldsymbol{v}_1,\ldots,\boldsymbol{v}_{n-1}$ *orthonormal with respect to g the system* $\boldsymbol{v}_1\times\ldots\times\boldsymbol{v}_{n-1},\boldsymbol{v}_1,\ldots,\boldsymbol{v}_{n-1}$ *is an orthonormal base at p. Moreover,* $\Omega(\boldsymbol{v}_1\times\ldots\times\boldsymbol{v}_{n-1},\boldsymbol{v}_1,\ldots,\boldsymbol{v}_{n-1}) = 1$, *so the base is positively oriented.*

Assume now that D is a bounded domain in R^n with a smooth boundary ∂D. Assume that the considered structures g and Ω are defined on $D\cup\partial D$. Then g restricts naturally to ∂D. We will denote the restriction by the same letter g. At the same time Ω induces the volume form $\Omega_{\partial D}$ on the boundary ∂D as follows. Since, by the assumption ∂D is a smooth hypersurface in R^n, there exist, at every $p\in\partial D$, exactly one unit outer vector $\boldsymbol{n}$, normal to the boundary at p. The normal vectors constitute a smooth vector field on ∂D. In the case ∂D is a piece-wise smooth only, the field is defined almost everywhere on ∂D what does not influence the integral. In each case the form $\Omega_{\partial D}$ is defined for almost every $p\in\partial D$ by

$$\Omega_{\partial D}(\boldsymbol{v}_1,\ldots,\boldsymbol{v}_{n-1}) = \Omega(\boldsymbol{n},\boldsymbol{v}_1,\ldots,\boldsymbol{v}_{n-1})$$

for $\boldsymbol{v}_1,\ldots,\boldsymbol{v}_{n-1}$ hooked at p and tangent to ∂D.

It is clear that $\Omega_{\partial D}$ defines the orientation on ∂D in the sense that a basis $\boldsymbol{v}_1,\ldots,\boldsymbol{v}_{n-1}$ of vectors hooked at p and tangent to ∂D is positively oriented if and only if $\Omega_{\partial D}(\boldsymbol{v}_1,\ldots,\boldsymbol{v}_{n-1}) > 0$. We call this orientation *the orientation induced on ∂D by the orientation of D.* One can show that:

An ordered orthonormal basis $\boldsymbol{v}_1,\ldots,\boldsymbol{v}_{n-1}$ *represents the orientation induced on ∂D by the orientation of D if and only if*

$$\boldsymbol{n} = \boldsymbol{v}_1\times\ldots\times\boldsymbol{v}_{n-1}.$$

One can also show that the restricted g and induced $\Omega_{\partial D}$ are then compatible on ∂D, i.e., they satisfy the conditions (a)-(g) modified to the suitable dimension (dim $\partial D = n\text{-}1$).

Let $\boldsymbol{X}$ be a smooth vector field on $D \cup \partial D$. The *divergence* of $\boldsymbol{X}$, denoted by div $\boldsymbol{X}$, is a function defined by

$$(\operatorname{div} \boldsymbol{X})\, \Omega = L_{\boldsymbol{X}}\, \Omega$$

where $L_{\boldsymbol{X}}$ is the Lie derivative in direction $\boldsymbol{X}$ (cf. [3], Appendix 6).

One can show that in the particular case $\Omega = \Omega_{can}$, div $\boldsymbol{X} = \partial X_1/\partial x_1 + \ldots + \partial X_n/\partial x_n$.

Some more advanced considerations on the divergence can also be found in [4].

Now we are ready to state:

The divergence theorem

$$\int_D \operatorname{div} \boldsymbol{X}\, \Omega = \int_{\partial D} g(X, n)\ \Omega_{\partial D}.$$

Other versions of the theorem and possible applications will be given.

References

[1] Spivak M, Calculus on manifolds, a modern approach to classical theorems of advanced calculus, Addison-Wesley Publishing Company, 1995.

[2] Pierzchalski A, Gradients: the ellipticity and the elliptic boundary conditions – a jigsaw puzzle, Folia Mathematica, Vol 19, No. 1, 2017, 65–83.

[3] Kobayashi S., Nomizu K., Foundations of Differetial Geometry, Vol I, Interscience Publishers, a division of John Wiley & Sons, New York –London, 1963.

[4] Kalina J., Kozłowski W., Pierzchalski A., On the geometry of a pair of foliations and a conformal invariant, to appear.

YOUNG MEASURES ASSOCIATED WITH SEQUENCES OF A CERTAIN CLASS OF M-OSCILLATING FUNCTIONS

Piotr Puchała

Department of Mathematics, Czestochowa University of Technology, Czestochowa, Poland
piotr.puchala@im.pcz.pl

Keywords: ***Young measures, m-oscillating functions, total slope, weak convergence***

The origin of the discovery of Young measures lie in the seeking the minima of integral functionals having non(quasi)convex integrands. One of the first examples concerning this type of optimization problems are attributed to Oscar Bolza and Laurence Chisholm Young. Namely, we want to minimize the functional of the form

$$J(v) = \int_0^1 \left[v^2 + \left(\left(\frac{dv}{dx} \right)^2 - 1 \right)^2 \right] dx, \tag{1}$$

where the function v vanishes at the ends of the interval. The functional J is bounded from below by the zero function, but it turns out that this infimum is never attained. The elements of the sequences minimizing the functional J are functions of highly oscillatory nature; they oscillate more and more wildly around the $\inf J$.

Contemporary formulation of this problem is as follows. We look for the infimum of the bounded from below functional of the form

$$J(v) = \int_\Omega f\big(x, v(x), \nabla v(x)\big)\, dx, \tag{2}$$

where:

- Ω is an open, bounded subset of $\mathbb{R}^n$ with sufficiently smooth boundary;
- v is an element of a suitable (usually Sobolev) space V of functions on Ω with values in a compact set $K \subset \mathbb{R}^m$;
- $f: \Omega \times \mathbb{R}^n \times \mathbb{R}^{mn} \to \mathbb{R} \cup \{+\infty\}$ is assumed to satisfy suitable regularity and growth conditions.

Laurence Chisholm Young proved in [5] that the weak* limits of the sequences of the form mentioned above are in general families of probability measures, nowadays called the *Young measures*. They are usually denoted

$$\nu = (\nu_x)_{x \in \Omega}, \tag{3}$$

where each ν_x is a regular countably additive probability measure on the set $K \subset \mathbb{R}^m$ (that is, it belongs to the Banach space $\mathrm{rca}^1(K)$).

There are several (not entirely equivalent, but not pairwise disjoint) approaches to Young measures. One of them, described in [4], relies on regarding Young measures as weakly* measure- valued mappings

$$\nu: \Omega \ni x \to \nu(x) \in \mathrm{rca}^1(K). \tag{4}$$

In the presentation we introduce a notion of a total slope of an oscillating function and a notion of m-oscillating function. We also state state the result which collectes most of the existing examples of homogeneous Young measures with densities into its special case.

References

[1] Puchała P., An elementary method of calculating an explicit form of Young measures in some special cases, Optimization 2014, vol. 63 No.9, 1419-1430.

[2] Puchała, P., A simple characterization of homogeneous Young measures and weak convergence of their densities, Optimization 2017, vol. 66 No.2, 197-203.

[3] Puchała P., Weak convergence of sequences of Young measures with densities, submitted.

[4] Roubíček T., Relaxation in Optimization Theory and Variational Calculus, Walter de Gruyter, Berlin, New York, 1997.

[5] Young L.C., Generalized curves and the existence of an attained absolute minimum in the calculus of variations, C. R. Soc. Sci. Lett. Varsovie, Classe III, 1937, 30, 212-234.

EFFECT OF THROAT GEOMETRY ON MIXING PHENOMENON IN VENTURI GAS MIXER USING OPENFOAM

Mathias Romańczyk

Department of Thermal Machinery, Czestochowa University of Technology, Czestochowa, Poland
mathias@imc.pcz.czest.pl

Keywords: **computational mechanics, mixing phenomena, Venturi effect, AFR analysis, pressure loss**

In this paper main focus will be paid on the physical analysis of the mixing process and the effect of throat geometry on the mixing phenomenon in Venturi gas mixer by determining the optimal ratio between throat diameter and it's length using the open source computational fluid dynamics simulation software OpenFOAM. The main task of a gas mixer is to mix the fuel (gas) with air in such a way, that in the gas engine optimal combustion takes place [1]. To provide an efficiency combustion process in the industrial gas engine, the Venturi mixer should be designed to allow the best possible mixing of the two components, air and fuel. Additionally it should be compact, with minimum of pressure loss, and moreover good suction pressure in the throat due to the Venturi principle. A lot of analyzes have been performed to improve the efficiency of the whole mixing process in a Venturi gas mixer [2, 3, 4]. However, the influence of some geometrical parameters have not been analyzed so far in detail, what is important especially for the manufacturers of such gas mixing devices. One of such important geometrical parameter was the throat length, how its length impacts the whole mixing process in a Venturi gas mixer. Therefore investigations were performed to determinate the optimal ratio between the throat diameter (which was set constantly on *Ø25mm*) and its length (from *100mm* → *200mm*) using the open source computational fluid dynamics simulation software OpenFOAM.

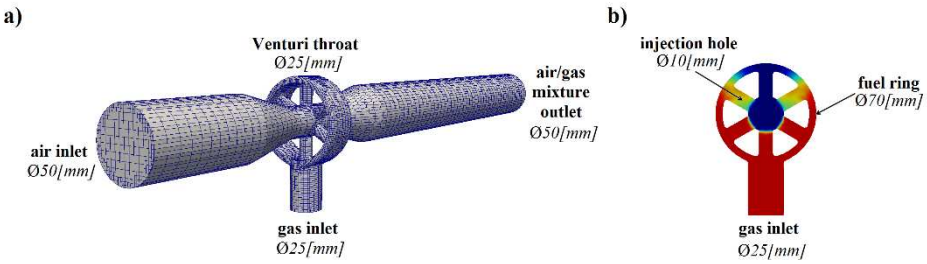

Fig. 1. Venturi gas mixer – a) dimensions – b) fuel ring with six injection holes

Three different ratios (*4:1, 6:1, 8:1*) has been investigated in this paper. Different throat lengths are the result of different diffuser angles and mixing characteristics at the outlet of the Venturi throat what has been presented in Figure 2.

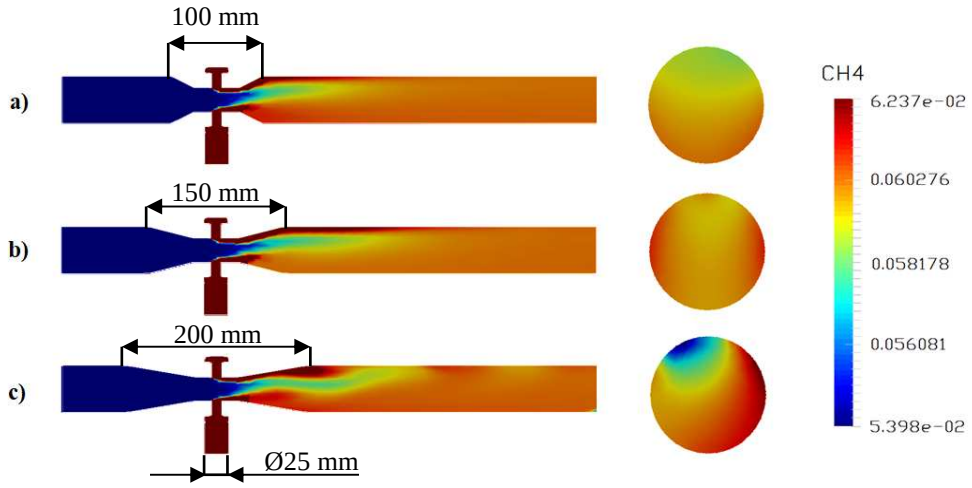

Fig. 2. Mixing traces and methane CH4 concentration distribution for different throat lengths – a) 100 mm (Ratio 4:1), b) 150 mm (Ratio 6:1), c) 200 mm (Ratio 8:1)

This numerical analysis showed that the throat geometry of a Venturi gas mixer influences significantly the mixing characteristics. Different diffuser angles causes different concentration distributions. As shown in Figure 2, the longest mixing trace appears for the greatest throat length → 200mm. Initially was expected, the longer the mixing trace, the better the mixing characteristic in the outlet of the Venturi gas mixer which turned out not to be true in this case analysis.

References

[1] Gorjibandpy M, Mehdi Kazemi Sangsereki, Computational Investigation of Air-Gas Venturi Mixer for Powered Bi-Fuel Diesel Engine. World Academy of Science, Engineering and Technology. International Journal of Mechanical, Aerospace, Industrial, Mechatronic and Manufacturing Engineering Vol:4, No:11, 2010.

[2] Danardono D, Ki-Seong Kim, Sun-Youp Lee, Jang-Hee Lee, Optimization the design of venturi gas mixer for syngas engine using three-dimensional CFD modeling. Journal of Mechanical Science and Technology 25 (9) 2285-2296, 2011.

[3] Romańczyk M, Elsner W, Numerical analysis for optimal localization of gas inlet in a Venturi mixer, 23rd International Conference Engineering Mechanics 2017, ISBN 978-80-2014-5497-2, Svratka, Czech Republic, 15-18 May 2017, 2017.

[4] Romańczyk M, Elsner W, Effect of Cylindrical Turbulators on the Mixing Process in Basic Venturi Gas Mixer Using OpenFOAM, III International Conference of Computational Methods in Engineering Science (CMES'18), DOI: 10.1051/matecconf/201925204004, Vol.252, 04004, 2019.

AN EXACT SOLUTION OF FRACTIONAL EULER-BERNULLI EQUATION WITH DIFFERENT TYPES OF BOUNDARY CONDITIONS

Jaroslaw Siedlecki [1]***, Tomasz Blaszczyk*** [2]

[1,2]*Department of Mathematics, Czestochowa University of Technology, Czestochowa, Poland*
[1]*jaroslaw.siedlecki@pcz.pl*, [2]*tomasz.blaszczyk@pcz.pl* ,

Keywords: **Euler-Bernoulli beam equation, fractional Caputo derivatives**

In this paper we studied the fractional Euler-Bernoulli beam equation including a composition of the left and right fractional Caputo derivative

$$ {}^{C}D_{L^-}^{\alpha}\ {}^{C}D_{0^+}^{\alpha}u(x)=F(x) \tag{1}$$

where

$$F(x)=\frac{f(x)}{\ell^{2(\alpha-2)}EI} \tag{2}$$

We analysed the equation (1) with three types of boundary conditions

$$u(0)=u'(0)=u(L)=u'(L)=0 \tag{3}$$

$$u(0)=u'(0)=u(L)=u''(L)=0 \tag{4}$$

$$u(0)=u'(0)=u''(L)=u'''(L)=0 \tag{5}$$

The differential equation is transformed into integral ones, using the assumed boundary conditions. Exact solutions received for each considered case of boundary conditions (3) – (5) contain the composition of the left and right Riemann-Liouville integral.

Case I. For boundary condition (3) we have the solution

$$\begin{aligned} u(x)=\frac{x^{\alpha}}{2L^{\alpha}}\Bigg[\left((\alpha+1)(\alpha-2)+\frac{1}{L}(\alpha-1)\big(x-(\alpha+1)L\big)\right)\left(I_{0^+}^{\alpha}I_{L^-}^{\alpha}F(x)\Big|_{x=L}\right) \\ -\frac{L}{\alpha}(x-L)\left(DI_{0^+}^{\alpha-1}I_{L^-}^{\alpha}F(x)\Big|_{x=L}\right)\Bigg]+I_{0^+}^{\alpha}I_{L^-}^{\alpha}F(x) \end{aligned} \tag{6}$$

Case II. For boundary condition (4) the solution has the following form

$$u(x)=\frac{x^{\alpha}}{\alpha\left(\alpha^{2}-1\right)L^{\alpha-1}}\Big[\Big(\left(\alpha^{2}-1\right)(\alpha-3)L$$
$$+(\alpha-1)(\alpha-2)\left(x-(\alpha+1)L\right)\Big)DI_{0^{+}}^{\alpha-1}I_{L^{-}}^{\alpha}F(x)\Big|_{x=L} \tag{7}$$
$$-L\Big(\left(\alpha+1\right)(2-\alpha)L+(\alpha-1)\left(x-(\alpha+1)L\right)\Big)D^{2}I_{0^{+}}^{\alpha-1}I_{L^{-}}^{\alpha}F(x)\Big|_{x=L}\Big]+I_{0^{+}}^{\alpha}I_{L^{-}}^{\alpha}F(x)$$

Case III. For boundary condition (5) we received the solution

$$u(x)-\frac{x^{\alpha}}{L^{\alpha}}\left[\left(\frac{\alpha x}{L}-\alpha-1\right)I_{0^{+}}^{\alpha}I_{L^{-}}^{\alpha}\ f^{*}(x)\Big|_{x=L}+(L-x)I_{0^{+}}^{\alpha-1}I_{L^{-}}^{\alpha}\ f^{*}(x)\Big|_{x=L}\right] \tag{8}$$
$$=I_{0^{+}}^{\alpha}I_{L^{-}}^{\alpha}\ f^{*}(x)$$

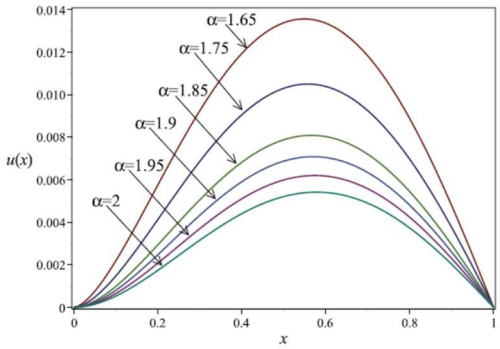

Fig. 1. The exact solution of Eq. (1) with boundary conditions (4) for the function *f(x)=1* and parameters $L = 1$, $\ell = 1$, $E = 1$, and $I = 1$.

References

[1] Blaszczyk T., Siedlecki J., Sun. HG., An exact solution of fractional Euler-Bernoulli equation for a beam with fixed-supported and fixed-free ends. Applied Mathematics and Computation, 396, 2021, 125932.

[2] Blaszczyk T., Analytical and numerical solution of the fractional Euler-Bernoulli beam equation, Journal of Mechanics of Materials and Structures, 12(1), 2017, 23-34.

SOME EXTENSIONS OF SEMANTIC MODELLING FOR SELECTED DOMAIN SPECIFIC LANGUAGES

William Steingartner [1]***, Valerie Novitzká*** [2]

[1,2]*Faculty of Electrical Engineering and Informatics, Technical University of Košice, Košice, Slovakia*
[1]*william.steingartner@tuke.sk,* [2]*valerie.novitzka@tuke.sk*

Keywords: **domain-specific languages, semantic methods, semantic modelling**

Professional programmers need to come to terms with the need to know several programming languages. On the one hand, knowledge of several languages can significantly increase the mental load on the programmer, on the other hand, all languages have similar syntactic structures, and semantics and the standard language library are a significant difficulty in mastering languages [1].

A Domain-Specific Language is a programming language with a higher level of abstraction. Unlike low-level languages, which are applicable across different domains, domain-specific languages (DSLs) specialize in a particular subject area [2]. One of the very nice examples of DSL is a battle management language, for which the semantic approach was formulated in [5]. DSLs are considered as small programming languages with some limited expressiveness. They are usually focused on a particular problem domain (possibly not Turing-complete) – for particular problems, a DSL could be a much more efficient tool than a general low-level language. In that sense, they provide more effective development than in general purpose languages. In practice, domain specific languages are often implemented as an embedded language into some another language. Furthermore, the semantics is then expressed in the host language [3].

We report here on a semantics of DSL expressing a robot coordination language—a language to help the robot get to the exit door. An introduction to this language and some basic ideas about formulating the denotational and operational semantics were published at [4].

In this contribution, we show how to formulate other semantic approaches for this kind of language and we show the semantic equivalence for the presented semantic methods.

Acknowledgments

This work was supported by:
(1) project KEGA 011TUKE-4/2020: “A development of the new semantic technologies in educating of young IT experts”; and

(2) Initiative project “Semantic Modeling of Component-Based Program Systems” under the bilateral program “Aktion Österreich – Slowakei, Wissenschafts- und Erziehungskooperation”.

References

[1] Kalyakin A., What are Domain Specific Languages? 1C as an example of a DSL. Online, https://1c-dn.com/blog/what-are-domain-specific-languages-1c-as-an-example-of-a-dsl, Accessed: 2021-03-14.

[2] Kollár J., Porubän J., Chodarev S., Modelovanie a generovanie softvérových architektúr, Technical University of Košice, Slovakia, 2012.

[3] Nielson H.R., Nielson F., Semantics with Applications: An Appetizer. Series Undergraduate Topics in Computer Science, Springer-Verlag London 2007.

[4] Horpácsi D., Kőszegi J., Formal Semantics, Lecture 13 – Domain Specific Languages, 2014, Online, https://regi.tankonyvtar.hu/hu/tartalom/tamop412A/2011-0052_05_formal_semantics, Accessed: 2021-03-14.

[5] Benčík M., Dedera L., Natural Semantics of Battle Management Languages, In: Proceedings of the 2019 Communication and Information Technologies – KIT (9th–11th October 2019, Vysoké Tatry, Slovakia), IEEE, 2019.

NUMERICAL SIMULATION OF THERMAL PHENOMENA DURING BUTT WELDING OF ALUMINUM ALLOY SHEETS

Jerzy Winczek [1]***, Mateusz Matuszewski*** [2]

[1,2]*Department of Technology and Automation, Czestochowa University of Technology, Czestochowa, Poland*
[1]*winczek@imipkm.pcz.pl*, [2]*matuszewski@itm.pcz.pl*

Keywords: **aluminium alloy, ANSYS, modelling, temperature field, welding**

The basis of welding processes is the generation of the appropriate temperature field by the heat source or sources. Therefore, the starting point for modelling and analyzing thermomechanical states during welding is always to adopt an appropriate model of the heat source and describe the temperature field [1-6].

In work, the modelling of a three-dimensional temperature field in a butt welded joints of two 6060 aluminium alloy sheets using FEM (Finite Element Method) is presented. Welding tests of single pass butt welded joint of 6060 aluminium alloy sheets were carried out using two methods (in the argon shield): GTA (Gas Tungsten Arc) and GMA (Gas Metal Arc).

In computation of temperature field, the Goldak's double ellipsoidal heat source model has been used [7]. The thermal-mechanical properties of the material were assumed to depend on the temperature. The Workbench, DesignModeler, Mechanical, Fluent and CFD-Post modules of the ANSYS program were used for numerical simulations [8-10]. The scheme of single-pass butt welding of aluminium alloy sheets is presented in Fig. 1.

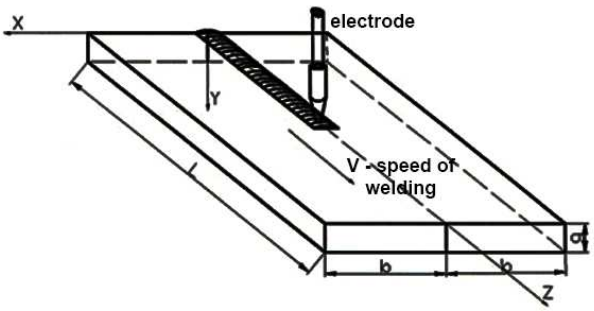

Fig. 1. The scheme of single-pass butt welding process

In the description of the geometry of joints, cube type elements were used, with density of grid in the heat affected zone. The parabolic shapes of face and root were assumed based on the literature and results of the experiment. The temperature distributions in cross-sections of welded joints as well as welding thermal cycles at selected points were analyzed.

In Fig. 2, the temperature distribution during welding of Al6060 alloy sheet with the GTA method at time t = 69 s from the beginning of welding in the cross-section is presented.

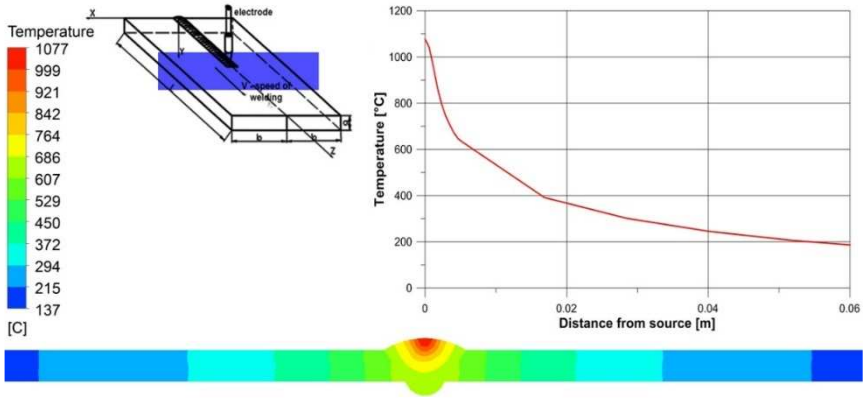

Fig. 2. Temperature distribution during welding of Al6060 alloy sheet with the GTA method at time *t* = 69 s from the beginning of welding in the cross-section

In turn, Fig. 3 shows the temperature distribution during welding of Al6060 alloy sheet with the GMA method at time *t* = 24 s from the beginning of welding in the cross-section.

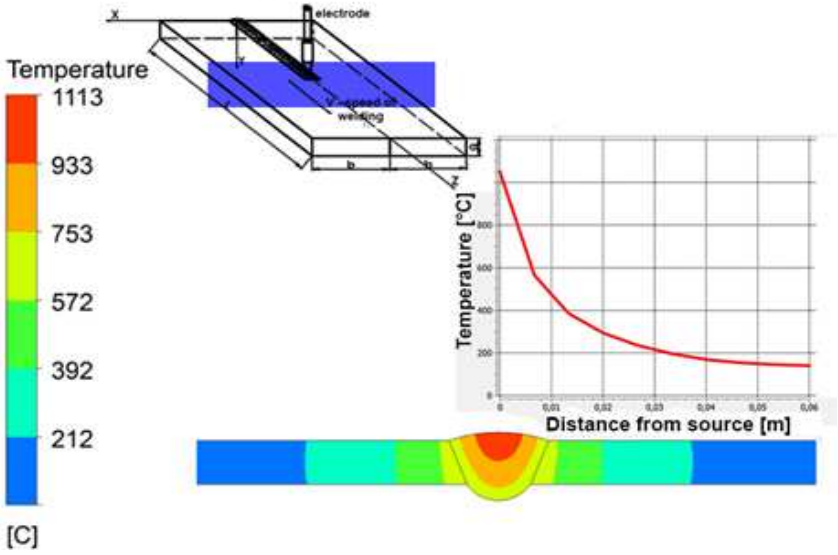

Fig. 3. Temperature distribution during welding of Al6060 alloy sheet with the GMA method at time *t* = 24 s from the beginning of welding in the cross-section

The results of numerical simulations were verified experimentally. The comparison of experimental and numerical simulations is presented in Fig. 4 (for GTA method) and Fig. 5 (for GMA method).

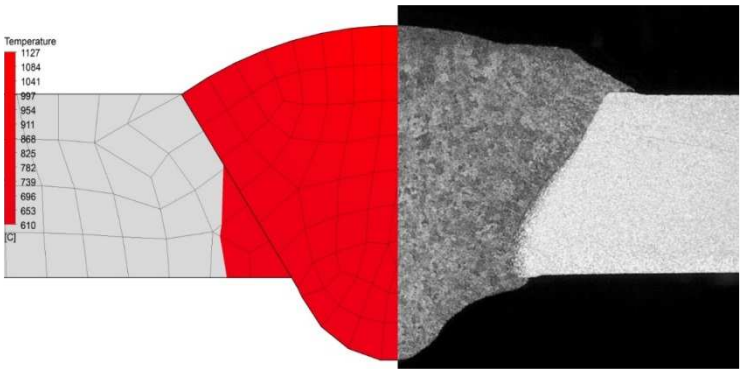

Fig. 4. The comparison of calculated fusion zone (left) to the metallographic tests (right) for GTA welding method

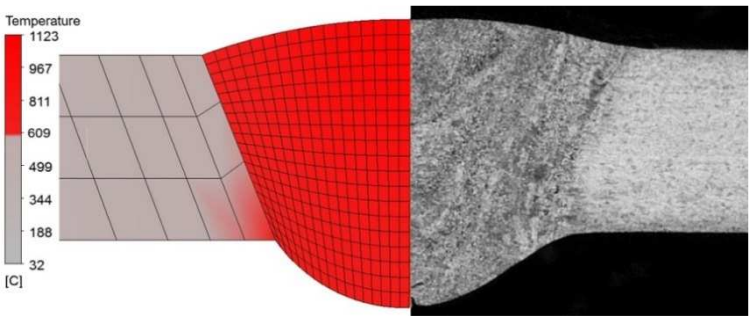

Fig. 5. The comparison of calculated fusion zone (left) to the metallographic tests (right) for GMA welding method

Comparison of calculated and obtained in the experiment the characteristic limits of heat affected zones showed satisfactory compatibility. The red color on the left shows the area in which we reached the temperature above the solidus where the material melts. The difference in dimensions obtained in the simulation with respect to experimental tests is below 5%.

Numerical simulations of the temperature field in welding processes for sheets made of aluminium alloys allowed to determine the fusion zone of welded sheets in the mentioned welding processes.

Numerical simulations of the temperature field in welding processes for sheets made of aluminium alloys:

- butt welded joint made with the GTA method (using a infusible (tungsten) electrode in the Argon shield with the addition of a deposited metal in the form of a wire),
- butt welded joint made with the GMA method (using a fusible electrode in the Argon shield),

allowed to determine the fusion zone of welded sheets in the mentioned processes.

The obtained results are the origin point for the calculation of strain and stress states in the welding processes considered in the paper.

References

[1] Parkitny R., Winczek J., Analytical solution of temporary temperature field in half-infinite body caused by moving tilted volumetric heat source, Int. J. Heat Mass Transf. 2013, 60, 469 – 479.

[2] Winczek J., Modeling of temperature field during multi-pass GMAW surfacing or rebuilding of steel elements taking into account the heat of the deposit metal, Appl. Sci., 2017, *7*(1), 6; doi:10.3390/app7010006, 1 – 19.

[3] Chen Q., Yang J., Liu X., Tang J., Huang B., Effect of the groove type when considering a thermometallurgical-mechanical model of the welding residual stress and deformation in an S355JR-316L dissimilar welded joints, J. Mater. Process. Technol., 2019, 45, 290–303.

[4] Kik T., Moravec J, Švec M., Experiments and numerical simulations of the annealing temperature influence on the residual stresses level in S700MC steel welded elements, Materials, 2020, 13, 5289. https://doi:10.3390/ma13225289

[5] Arsić D., Ivanović B.I., Sedmak A.S., Lazić M.M., Kalaba D.V, Čeković I.R., Ratković N.R., Experimental and numerical study of temperature field during hard-facing of different carbon steels, Therm. Sci. 2020, 24, No. 3B, 2233–2241.

[6] Kik T., Górka J., Kotarska A., Poloczek T., Numerical verification of tests on the influence of the imposed thermal cycles on the structure and properties of the S700MC heat-affected zone, Metals 2020, 10, 974. https://doi:10.3390/met10070974

[7] Goldak J., Chakravarti A., Bibby M., A new finite element model for welding heat sources, Metall. Mater. Trans. B, 1984, 15, 299–305.

[8] Ansys. Theory Reference. 11-th ed., Ansys Inc., Canosburg 1999.

[9] Moaveni S., Finite element analysis: theory and application with ANSYS, 3 ed., Pearson Prentice Hall, New York 2008.

[10] Madenci E., Guven I., The finite element method and applications in engineering using ANSYS®, Springer, New York 2006.

LOCALLY DEFINED OPERATORS IN THE SPACES OF FUNCTIONS OF BOUNDED JORDAN VARIATION

Małgorzata Wróbel

Department of Mathematics, Czestochowa University of Technology, Czestochowa, Poland
malgorzata.wrobel@im.pcz.pl

Keywords: **locally defined operator, Nemytskij composition operator, Jordan type variation, locally bounded operator, uniformly bounded operator**

Let $I=[a,b]$ be a closed interval of real axis ($a,b\in R,\ a<b$). The function $\phi: I\to R$ is said to be *of bounded variation on the interval* $I=[a,b]$, briefly $f\in BV(I)$, if the quantity

$$V(\phi,I)=\sup_{\pi}\sum_{i=1}^{m}|\phi(x_i)-\phi(x_{i-1})|,$$

where the supremum is taken over all partitions of the interval I, is finite. We will write $CBV(I)\,\text{for}\,\mathrm{C(I)}\cap BV(I)\,\text{where}\,\mathrm{C(I)}$ denotes the family of real continuous functions defined on I.

Definition. An operator $\mathrm{K}: CBV(I)\to CBV(I)$ is said to be *locally defined*, if for every open interval $J\subset R$ and for all functions $\phi,\varphi\in CBV(I)$ the following implication holds true:

$$\phi|_J=\varphi|_J \Rightarrow K(\phi)|_J=K(\varphi)|_J.$$

Theorem 1. If a locally defined operator K maps $CBV(I)$ into itself, then it is a Nemytskij composition operator, i.e., there exists a unique function $h: I\times R\to R$ such that

$$K(\phi)(x)=h(x,\phi(x)),\qquad \phi\in CBV(I),\qquad (x\in I). \tag{1}$$

In the talk we also characterize locally defined operators acting between the spaces of functions of bounded variation under the additional assumption that they are locally bounded or uniformly bounded.

We say that a function $f:[0,1]\times R\to R$ satisfies a condition (ii) if for every $\mathrm{r}>0$ there exists a constant $M_r>0$ such that for every $k\in N$, every partition

$0 = t_1 < ... < t_k \le 1$ of the interval $I = [0,1]$ and every finite sequence $u_0, u_1, .., u_k \in [-r, r]$ with $\sum_{i=1}^{k} |u_i - u_{i-1}| \le r,$ the following inequalities hold:

$$\sum_{i=1}^{k} |f(t_i, u_i) - f(t_{i-1}, u_i)| \le M_r \quad \text{and} \quad \sum_{i=1}^{k} |f(t_{i-1}, u_i) - f(t_{i-1}, u_{-1i})| \le M_r .$$

The Nemytskij composition operator $\mathrm{K} : \mathrm{C}BV(I) \to CBV(I)$ is said to be *locally bounded*, if the image of each ball $K(B_{BV}(0, M))$ is bounded in $\mathrm{C}BV(I)$.

Theorem 2. If a locally defined operator K maps $CBV(I)$ into itself and is locally bounded then there exists a unique function $h : I \times R \to R$ satisfying condition (ii) such that (1) is fulfilled.

Conversely, if an operator $K : R^I \to R^I$ is defined by (1) for some function $h : I \times R \to R$ satisfying condition (ii) of Theorem 2, then the operator K maps $CBV(I)$ into itself and is locally defined and locally bounded.

Theorem 3. If a locally defined operator K (with continuous with respect to the second variable generating function $h(x,\cdot) : R \to R$) maps $CBV(I)$ into itself and is uniformly bounded, then there exist $\alpha(\cdot) \in CBV(I)$ and $\beta(\cdot) \in CBV(I)$ such that

$$K(\phi)(x) = \alpha(x)\phi(x) + \beta(x), \qquad \phi \in CBV(I), \qquad (x \in I).$$

As a corollary we get that every Lipschitzian or uniformly continuous locally defined operator acting between the spaces of functions of bounded Jordan variation has an affine (in the second variable) generator.

References

[1] Bugajewska D., Bugajewski D., Kasprzak P., Maćkowiak P., Nonautonomous superposition operators in the spaces of functions of bounded variation, Topol. Methods Nonlinear Anal., 2016, 48(2), 637-666.

[2] Matkowski J., Uniformly bounded composition operators between general Lipschitz functions normed spaces, Topol. Methods Nonlinear Anal. 2011, 38(2), 395-406.